

Robustness of error-suppressing entangling gates in cavity-coupled transmon qubits

Xiu-Hao Deng, Edwin Barnes, and Sophia E. Economou
Department of Physics, Virginia Tech, Blacksburg, Virginia 24061, USA

Superconducting transmon qubits comprise one of the most promising platforms for quantum information processing due to their long coherence times and to their scalability into larger qubit networks. However, their weakly anharmonic spectrum leads to spectral crowding in multiqubit systems, making it challenging to implement fast, high-fidelity gates while avoiding leakage errors. To address this challenge, we have developed a protocol known as SWIPHT, which yields smooth, simple microwave pulses designed to suppress leakage without sacrificing gate speed through spectral selectivity. Here, we demonstrate that SWIPHT systematically produces two-qubit gate fidelities for cavity-coupled transmons in the range 99.6%-99.9% with gate times as fast as 23 ns. These high fidelities persist over a wide range of qubit frequencies and other system parameters that encompasses many current experimental setups and are insensitive to small deformations in the optimized pulse shape. Our results are obtained from full numerical simulations that include current experimental levels of relaxation and dephasing.

Rapid progress in the coherence and controllable coupling of superconducting qubits over the past decade has made them a frontrunner in the quest for viable quantum computing platforms [1–4]. High fidelity single- and multi-qubit operations [5–9], as well as initial demonstrations of algorithms and error-correcting codes [10–14], have been implemented in several multi-qubit devices, and coherence times on the order of several tens of microseconds and above are now achieved regularly [15–20]. Perhaps the most promising of these are transmon qubits, in which insensitivity to charge noise is achieved by reducing the capacitive energy relative to the Josephson energy through the use of a large shunt capacitor, leading to a flattening of the charge dispersion of the energy levels [21–23].

There are two general approaches to implementing two-qubit gates in superconducting qubits. For tunable qubits such as 2D transmons [21] or Xmons [23], DC magnetic fields are used to set qubit energies and other circuit parameters. In many systems, such fields are also used to implement gates by temporarily bringing the system to a special parameter regime (e.g., a two-qubit resonance), where it is held idle until different states accumulate the relative phases appropriate for a desired operation [24, 24–26]. The main disadvantages of this approach are the reliance on flux-tunable qubits, which can have reduced coherence times due to flux noise [27], the risk of interacting with other energy levels in the system during tuning, and additional circuit and control complexity due to on-chip tunable flux controls or couplers which support dynamical tunability.

The second general approach to gate implementation is to drive one or more qubits with modulated AC microwave pulses. This method leads to less noise since the qubit energies are held fixed, and it is the only option for systems with non-tunable qubits [28–32]. The primary challenge with this approach stems from spectral crowding: a system of several coupled, weakly anharmonic qubits such as transmons possesses a dense energy

spectrum with many closely spaced transitions.

The impact of spectral crowding on microwave-based gate operations can be understood from energy-time uncertainty. Faster gates are generally preferred since they allow for faster algorithms. However, faster pulses have broader bandwidth and thus tend to excite more transitions. This causes unintended excitation of transitions that are nearly degenerate with the target transition(s), leading to phase and leakage errors. On the other hand, using spectrally narrower, slower pulses to avoid this problem increases exposure to relaxation and decoherence. To date, there have been several works that address this problem in the context of single-qubit gates by devising pulses that avoid the harmful transitions, either by numerical pulse shaping [33] or by engineering the pulse spectrum to contain sharp holes at the frequencies of the unwanted transitions [34–36]. The design of microwave control protocols that combat leakage in the case of two-qubit entangling gates has remained an open problem. Recent experiments implementing microwave-driven two-qubit entangling gates in transmon devices have reported gate times and fidelities ranging from 300 – 500 ns and 87 – 97% [6, 13, 17].

Instead of attempting to avoid harmful unwanted transitions, two of us proposed a new protocol called SWIPHT [38] to achieve fast and high-fidelity two-qubit gates by purposely driving the nearest harmful transition and incorporating its dynamics into the gate design. In particular, the driving field is engineered so that the harmful transition subspace undergoes trivial cyclic evolution. This minimizes leakage errors and significantly enhances gate fidelities without resorting to slow, spectrally selective pulses. While Ref. [38] developed the SWIPHT protocol and numerically demonstrated its efficacy, a full examination of its robustness to parameter variations and its performance under decoherence and relaxation has yet to be carried out.

In this paper, we fill this gap by providing a detailed investigation of the robustness of the SWIPHT protocol

for two-qubit CNOT gates. We show that there exist wide fidelity plateaus in the qubit-frequency landscape where the fidelity remains above 99.9%. We also find that with our method, we are able to maintain the CNOT fidelity at 99.9% while decreasing the gate time to tens of nanoseconds by exploiting resonances between ground and excited state transitions. We further demonstrate the robustness of these results to decoherence and relaxation, variations in qubit-cavity couplings and qubit frequencies, and pulse deformations using experimental realistic decay times and parameter uncertainties.

We focus on a superconducting circuit where two transmons are coupled to a superconducting cavity. The Hamiltonian of this system is

$$H_0 = \omega_c a^\dagger a + \sum_{\ell=1,2} [\omega_\ell b_\ell^\dagger b_\ell + \frac{\alpha}{2} b_\ell^\dagger b_\ell (b_\ell^\dagger b_\ell - 1) + g_\ell (a^\dagger b_\ell + a b_\ell^\dagger)]. \quad (1)$$

Here $a^\dagger(a)$, $b_{1,2}^\dagger(b_{1,2})$ are creation (annihilation) operators for the cavity and the transmons, respectively, $\omega_{1,2}$ denote the energy splittings between the first excited state and ground state for each transmon, α is the anharmonicity (assumed to be the same for both transmons), and $g_{1,2}$ are the coupling strengths between each transmon and the cavity. Working in the Fock basis $\{|n, i, j\rangle\}$, where n is the number of cavity photons, and i, j denote the energy levels of transmon 1 and 2, respectively, we diagonalize H_0 to obtain the dressed eigenstates. In the dispersive regime and with $g_{1,2} \ll \{\omega_c, \omega_{1,2}\}$, each dressed state has a large overlap with one of the bare Fock states; hence, we use n, i, j to denote the dressed states, but with an additional tilde: $\{|n, i, j\rangle\}$.

We define our computational two-qubit states to be the dressed states $\{|\widetilde{000}\rangle, |\widetilde{001}\rangle, |\widetilde{010}\rangle, |\widetilde{011}\rangle\}$, which are very close to the bare states, $\{|000\rangle, |001\rangle, |010\rangle, |011\rangle\}$, for typical system parameters. The splittings between the bare states $|000\rangle, |001\rangle$ and between $|010\rangle, |011\rangle$ are equal, as are those between $|000\rangle, |010\rangle$ and between $|001\rangle, |011\rangle$. These degeneracies are slightly broken in the dressed states due to the finite couplings $g_{1,2}$, allowing one to perform two-qubit entangling gates by driving only one transition, e.g., driving the $|\widetilde{000}\rangle \leftrightarrow |\widetilde{010}\rangle$ transition can implement a CNOT gate:

$$\text{CNOT} = e^{i\phi_a} |\widetilde{000}\rangle \langle \widetilde{010}| + e^{i\phi_b} |\widetilde{010}\rangle \langle \widetilde{000}| + e^{i\phi_c} |\widetilde{001}\rangle \langle \widetilde{001}| + e^{i\phi_d} |\widetilde{011}\rangle \langle \widetilde{011}|. \quad (2)$$

Here, we generalize the standard CNOT by including arbitrary phases ϕ_μ ; this generalized CNOT is locally equivalent to the standard one and is maximally entangling.

The CNOT gate in Eq. (2) can be implemented by driving only the first transmon with a microwave π -pulse that is resonant with the $|\widetilde{000}\rangle \leftrightarrow |\widetilde{010}\rangle$ transition. The total Hamiltonian is then

$$\mathcal{H}(t) = H_0 + b_1 \Omega(t) e^{i\omega_p t} + b_1^\dagger \Omega(t) e^{-i\omega_p t}, \quad (3)$$

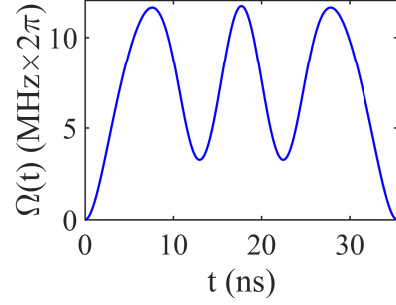


FIG. 1: Pulse envelope from Ref. [38] that implements a CNOT gate in 35.4 ns with $\omega_1 = 6.2$ GHz, $\omega_2 = 6.8$ GHz, $\omega_c = 7.15$ GHz, $\eta = 350$ MHz, $g_{1,2} = 250$ MHz.

where $\Omega(t)$ and ω_p are the pulse envelope and frequency, respectively. The simplest way to ensure that this transition is the only one excited by the pulse is to use a very narrowband pulse—an approach which necessarily leads to long gate times. To avoid making this sacrifice in gate speed, we instead employ the SWIPHT method [38] to remove the effects of inadvertently driving unwanted transitions without resorting to spectrally narrow, slow pulses. For typical experimental values of the qubit-cavity couplings $g_{1,2}$, there is exactly one nearest “harmful” transition, namely the $|\widetilde{001}\rangle \leftrightarrow |\widetilde{011}\rangle$ transition, which competes with the target transition, $|\widetilde{000}\rangle \leftrightarrow |\widetilde{010}\rangle$. The SWIPHT protocol calls for purposely driving this transition in such a way that the net evolution operator in this subspace is proportional to an identity operation.

In the computational two-qubit subspace spanned by the states $|\widetilde{000}\rangle, |\widetilde{010}\rangle, |\widetilde{001}\rangle, |\widetilde{011}\rangle$, the Hamiltonian of the coupled transmon-cavity system including driving takes the approximate form

$$H_{cs} \approx \begin{pmatrix} -E/2 - \epsilon & \Omega(t)e^{i\omega_p t} & 0 & 0 \\ \Omega(t)e^{-i\omega_p t} & E/2 - \epsilon & 0 & 0 \\ 0 & 0 & -(E - \delta)/2 & \Omega(t)e^{i\omega_p t} \\ 0 & 0 & \Omega(t)e^{-i\omega_p t} & (E - \delta)/2 \end{pmatrix}, \quad (4)$$

where E is the energy splitting between $|\widetilde{000}\rangle$ and $|\widetilde{010}\rangle$, and $E - \delta$ is the splitting between $|\widetilde{001}\rangle$ and $|\widetilde{011}\rangle$. We have shifted the overall energy by $-E/2 - \epsilon$, where $\epsilon + \delta/2$ is the energy of state $|\widetilde{001}\rangle$. We denote the pulse duration by τ_p . To implement a SWIPHT CNOT gate, we set $\omega_p = E$ and engineer $\Omega(t)$ such that the evolution operator generated by H_{cs} coincides with the CNOT gate given in Eq. (2) with $\phi_\mu = 0$. Matching the form of the upper left 2×2 subspace requires the area of the pulse to be given by $\int_0^{\tau_p} dt \Omega(t) = \pi/2$, as is consistent with a π -pulse.

Engineering the evolution operator in the lower right 2×2 subspace to be an identity operation at time $t = \tau_p$ is more challenging since it is not possible to analytically solve the Schrödinger equation for an off-resonant

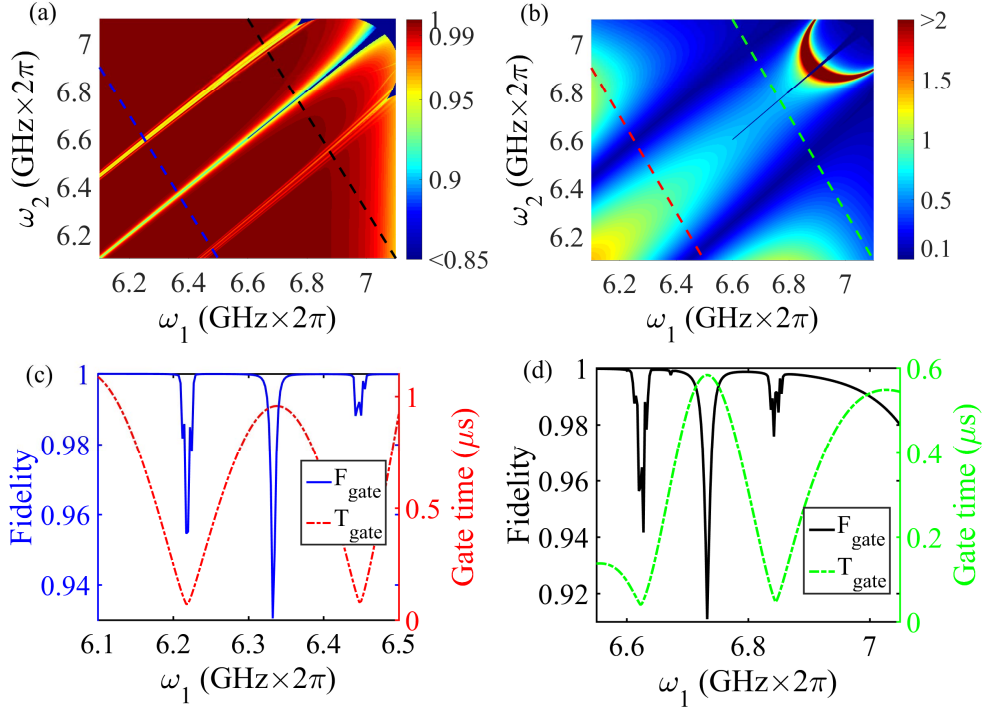


FIG. 2: (a) CNOT fidelity versus qubit frequencies. (b) Gate time (μs) versus qubit frequencies. $g_{1,2} = 100$ MHz, while all other parameters are as in Fig. 1. Cross-section plots for the four dashed lines are shown in (c) and (d) with corresponding colors.

pulse with arbitrary envelope $\Omega(t)$. As described in Ref. [38], we can overcome this difficulty by making use of a partial-reverse engineering formalism introduced in Refs. [39, 40]. In Ref. [38], this formalism was used to obtain the pulse shown in Fig. 1, which implements a CNOT gate with fidelity $> 99\%$ in 35.4 ns. The duration of the pulse is given by $\tau_p = 5.87/|\Delta|$, where $\Delta = \omega_p - (E - \delta)$ is the detuning of the pulse relative to the harmful transition. For $\omega_p = E$ we have $\Delta = \delta$, and thus τ_p depends on the system parameters through the dependence on the transition frequency difference δ . For the parameters considered in Ref. [38] (summarized in the caption of Fig. 1), $\delta = 26.4$ MHz.

First, we study the dependence of the CNOT fidelity and gate speed on the transmon frequencies. For the moment, we neglect relaxation and dephasing, although these effects will be included below. In this case, we define the gate fidelity as in Ref. [41], which accounts for leakage outside the computational two-qubit subspace:

$$\mathcal{F}^{\text{gate}} = \frac{1}{20} [\text{Tr}(MM^\dagger) + |\text{Tr}(M)|^2], \quad (5)$$

where $M = U_{\text{ideal}}U^\dagger$, and U is the actual evolution operator, while U_{ideal} is the target gate operation, here taken as the CNOT gate defined in Eq. (2). For each set of system parameters, we optimize over the phases ϕ_μ . Our numerical results are shown in Fig. 2. The most important features of Fig. 2(a) are the large plateaus where $\mathcal{F}^{\text{gate}}$ is well above 0.999 (dark red); these occur in re-

gions where $\omega_{1,2}$ are detuned from the three sharp linear features evident in the figure. The central feature corresponds to the qubit-qubit resonance, $\omega_1 = \omega_2$, while the two “secondary” resonances occur where $\omega_1 = \omega_2 \pm \eta$, corresponding to the $|0\rangle \leftrightarrow |1\rangle$ transition of one qubit becoming degenerate with the $|1\rangle \leftrightarrow |2\rangle$ transition of the other. Near these resonances, additional harmful transitions become important, causing a decrease in fidelity. This figure also exhibits an asymmetry between the dependencies on $\omega_{1,2}$ caused by the fact that only transmon 1 is driven. Since the high-fidelity plateau is broader for $\omega_1 < \omega_2$, we see that it is more advantageous to drive the transmon that is further detuned from the cavity.

Fig. 2(b) reveals that there is significant overlap between the high-fidelity plateaus and the parameter regions where the gate times are below 150 ns (blue). Interestingly, the fastest pulses occur near the secondary resonances. These resonances give rise to a larger splitting, δ , between the target and harmful transitions, which in turn reduces the SWIPT gate time since $\tau_p \sim 1/|\delta|$. Further details can be found in [42]. Figs. 2(c),(d) show the CNOT fidelity and gate time along two one-dimensional slices in qubit-frequency space. Importantly, we see that while the fidelity quickly increases up to above 0.999 as ω_1 is tuned away from a secondary resonance, the gate time increases more slowly. Thus, the best combination of low gate time and high fidelity is achieved when the system lies close to a secondary resonance. From Fig. 2(d), which shows a slice closer to the cavity frequency, $\omega_c = 7.15$

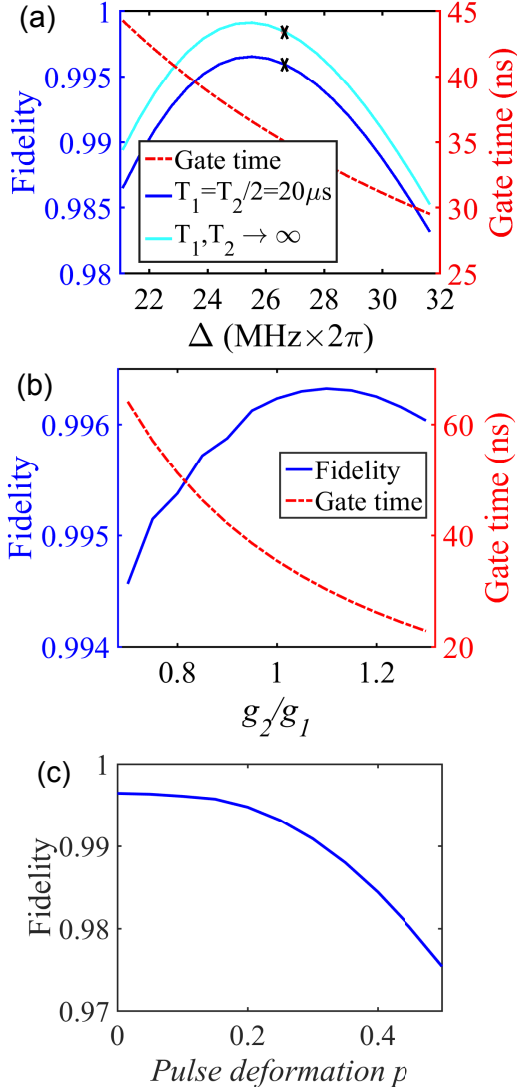


FIG. 3: (a) Fidelity versus detuning Δ for same system parameters as in Fig. 1. Cyan line is the fidelity for noiseless case while blue line is for $T_1 = T_2/2 = 20\mu\text{s}$. The black crosses indicate $\Delta = \delta$. Dashed red line shows gate time. (b) Fidelity and gate time versus g_2/g_1 for $g_1 = 250\text{ MHz}$, $T_1 = T_2/2 = 20\mu\text{s}$. All other parameters are as in Fig. 1. (c) Fidelity versus degree of pulse deformation from Eq. (8).

GHz, we in fact see that as ω_1 is reduced, the gate time saturates at around 150 ns while the fidelity continues to improve.

Next, we evaluate the performance of our gate in the presence of relaxation and decoherence by solving the Lindblad equation:

$$\dot{\rho} = i[\rho, \mathcal{H}(t)] + \sum_{\ell=1,2} \left(\frac{1}{T_1} \mathcal{D}[b_\ell] + \frac{1}{2T_2} \mathcal{D}[b_\ell^\dagger b_\ell] \right), \quad (6)$$

with $\mathcal{D}[L] = L\rho L^\dagger - \frac{1}{2}\{L^\dagger L, \rho\}$. The first Lindblad term corresponds to qubit relaxation (time scale T_1), while the second corresponds to decoherence (time scale T_2) caused

by charge fluctuations [21, 22]. We have neglected cavity decay in our simulation because its time scale is typically much larger than T_1 and T_2 and because our gate scheme causes minimal cavity excitation. With noise terms included, $\mathcal{F}^{\text{gate}}$ is no longer a suitable definition of fidelity, and we instead perform quantum state tomography. We prepare 16 input states in total, chosen from the set $\{|0\rangle, |1\rangle, (|0\rangle + |1\rangle)/\sqrt{2}, (|0\rangle + i|1\rangle)/\sqrt{2}\}$ for each qubit. We calculate the average fidelity, defined as

$$\mathcal{F} = \frac{1}{16} \sum_j \text{Tr}(\sqrt{\rho_{ideal}^j} \rho_{sim}^j \sqrt{\rho_{ideal}^j}) \quad (7)$$

where ρ_{ideal}^j is the ideal target state, while ρ_{sim}^j is the final density matrix obtained by solving Eq. (6).

With this definition of fidelity, we first study its dependence on the detuning of the pulse relative to the harmful transition, Δ . Fig. 3(a) shows this dependence with and without noise, where it is clear that a slight detuning away from the idealized value based on H_{cs} ($\Delta = \delta = 26.4\text{ MHz}$) down to $\Delta = 25.5\text{ MHz}$ brings the fidelity up to 0.9991 without noise or up to 0.9963 with noise for typical experimental values of T_1, T_2 . The figure also shows that this improvement comes with a slight increase in the gate time from 35.4 ns up to 36.6 ns. In [42], we show the dependence of the fidelity on T_1, T_2 for the optimized pulse with $\tau_p = 36.6\text{ ns}$, where we find that $\mathcal{F} \geq 0.995$ for $T_2 = 2T_1 \geq 7\mu\text{s}$. We also examine the performance of our gate for several sets of measured parameter values taken from recent experimental works.

In a real setup, the qubit-cavity coupling strengths g_1, g_2 may differ. Fig. 3(b) shows that the fidelity remains > 0.995 even when the couplings differ by more than 20%. We also find that further optimization of the gate is possible if the coupling of the undriven transmon (here g_2) is tuned to be slightly larger than the other (g_1). The figure further shows that the gate time is simultaneously reduced to as low as 23 ns while the fidelity remains above 0.996 with this adjustment.

In Fig. 3(c), we show the sensitivity of the results to Gaussian-type pulse deformations, which we incorporate by modifying the pulse according to

$$\Omega(t) = (1-p) * \Omega_{\text{SWIPT}}(t) + p * \Omega_{\text{Gaussian}}(t), \quad (8)$$

where $\Omega_{\text{SWIPT}}(t)$ is the pulse shown in Fig. 1, and p varies from 0 to 0.5. The Gaussian pulse is chosen to have duration and area equal to the SWIPT pulse. Pulse shapes for different values of p , along with a comparison of our SWIPT pulse against a pure Gaussian pulse of equal duration, are shown in [42]. Fig. 3(c) shows that the gate performance is essentially unchanged for deformations up to the 10% level, further highlighting the robustness of our gate.

In conclusion, we have shown that the SWIPT method can produce CNOT gates in cavity-coupled transmon systems with fidelities well above 99.5% and gate

times below 30 ns even when realistic levels of decoherence, relaxation, and parameter uncertainties are taken into account. Our work is of immediate use to ongoing experimental efforts to optimize the performance of transmon systems operated with microwave control.

-
- [1] J. Clarke and F. K. Wilhelm, *Nature* **453**, 1031 (2008).
- [2] J. Q. You and F. Nori, *Nature* **474**, 589 (2011).
- [3] M. H. Devoret and R. J. Schoelkopf, *Science* **339**, 1169 (2013).
- [4] J. M. Martinis and A. Megrant, arXiv:1410.5793 (2014).
- [5] J. M. Chow, J. M. Gambetta, A. D. Corcoles, S. T. Merkel, J. A. Smolin, C. Rigetti, S. Poletto, G. A. Keefe, M. B. Rothwell, J. R. Rozen, et al., *Phys. Rev. Lett.* **109**, 060501 (2012).
- [6] J. M. Chow, J. M. Gambetta, A. W. Cross, S. T. Merkel, C. Rigetti, and M. Steffen, *New J. Phys.* **15**, 115012 (2013).
- [7] R. Barends, J. Kelly, A. Megrant, A. Veitia, D. Sank, E. Jeffrey, T. C. White, J. Mutus, A. G. Fowler, B. Campbell, et al., *Nature* **508**, 500 (2014).
- [8] L. DiCarlo, M. D. Reed, L. Sun, B. R. Johnson, J. Chow, J. M. Gambetta, L. Frunzio, S. M. Girvin, M. H. Devoret, and R. J. Schoelkopf, *Nature* **467**, 574 (2010).
- [9] A. Fedorov, L. Steffen, M. Baur, M. P. da Silva, and A. Wallraff, *Nature* **481**, 170 (2012).
- [10] L. DiCarlo, J. M. Chow, J. M. Gambetta, L. S. Bishop, D. I. S. B. R. Johnson, J. Majer, A. Blais, L. Frunzio, S. M. Girvin, and R. J. Schoelkopf, *Nature* **460**, 240 (2009).
- [11] M. Mariantoni, H. Wang, T. Yamamoto, M. Neeley, R. C. Bialczak, Y. Chen, M. Lenander, E. Lucero, A. D. OConnell, D. Sank, et al., *Science* **334**, 61 (2011).
- [12] E. Lucero, R. Barends, Y. Chen, J. Kelly, M. Mariantoni, A. Megrant, P. O'Malley, D. Sank, A. Vainsencher, J. Wenner, et al., *Nat. Phys.* **8**, 719 (2012).
- [13] J. M. Chow, J. M. Gambetta, E. Magesan, S. J. Srinivasan, A. W. Cross, D. W. Abraham, N. A. Masluk, B. R. Johnson, C. A. Ryan, and M. Steffen, *Nat. Commun.* **5**, 4015 (2014).
- [14] M. D. Reed, L. DiCarlo, S. E. Nigg, L. Sun, L. Frunzio, S. M. Girvin, and R. J. Schoelkopf, *Nature* **482**, 382 (2012).
- [15] D. C. McKay, S. Filipp, A. Mezzacapo, E. Magesan, J. M. Chow, and J. M. Gambetta, *Phys. Rev. Applied* **6**, 064007 (2016).
- [16] S. Sheldon, L. S. Bishop, E. Magesan, S. Filipp, J. M. Chow, and J. M. Gambetta, *Phys. Rev. A* **93**, 012301 (2016).
- [17] A. Corcoles, E. Magesan, S. J. Srinivasan, A. W. Cross, M. Steffen, J. M. Gambetta, and J. M. Chow, *Nat. Commun.* **6**, 6979 (2015).
- [18] Y. Liu, S. Shankar, N. Ofek, M. Hatridge, A. Narla, K. Sliwa, L. Frunzio, R. J. Schoelkopf, and M. H. Devoret, *Phys. Rev. X* **6**, 011022 (2016).
- [19] C. Bultink, M. Rol, T. O'Brien, X. Fu, B. Dikken, R. Vermeulen, J. de Sterke, A. Bruno, R. Schouten, and L. DiCarlo, arXiv preprint arXiv:1604.00916 (2016).
- [20] S. Berger, M. Pechal, P. Kurpiers, A. Abdumalikov, C. Eichler, J. Mlynek, A. Shnirman, Y. Gefen, A. Wallraff, and S. Filipp, *Nat. Commun.* **6** (2015).
- [21] J. Koch, T. M. Yu, J. Gambetta, A. A. Houck, D. I. Schuster, J. Majer, A. Blais, M. H. Devoret, S. M. Girvin, and R. J. Schoelkopf, *Phys. Rev. A* **76**, 042319 (2007).
- [22] L. S. Bishop, arXiv preprint arXiv:1007.3520 (2010).
- [23] R. Barends, J. Kelly, A. Megrant, D. Sank, E. Jeffrey, Y. Chen, Y. Yin, B. Chiaro, J. Mutus, C. Neill, et al., *Phys. Rev. Lett.* **111**, 080502 (2013).
- [24] T. Yamamoto, M. Neeley, E. Lucero, R. Bialczak, J. Kelly, M. Lenander, M. Mariantoni, A. OConnell, D. Sank, H. Wang, et al., *Phys. Rev. B* **82**, 184515 (2010).
- [25] R. Bialczak, M. Ansmann, M. Hofheinz, M. Lenander, E. Lucero, M. Neeley, A. OConnell, D. Sank, H. Wang, M. Weides, et al., *Phys. Rev. Lett.* **106**, 060501 (2011).
- [26] A. Dewes, F. Ong, V. Schmitt, R. Lauro, N. Boulant, P. Bertet, D. Vion, and D. Esteve, *Phys. Rev. Lett.* **108**, 057002 (2012).
- [27] F. Yoshihara, K. Harrabi, A. Niskanen, Y. Nakamura, and J. Tsai, *Phys. Rev. Lett.* **97**, 167001 (2006).
- [28] H. Paik, A. Mezzacapo, M. Sandberg, D. McClure, B. Abdo, A. Corcoles, O. Dial, D. Bogorin, B. Plourde, M. Steffen, et al., *Phys. Rev. Lett.* **117**, 250502 (2016).
- [29] S. Poletto, J. M. Gambetta, S. T. Merkel, J. A. Smolin, J. M. Chow, A. Corcoles, G. A. Keefe, M. B. Rothwell, J. Rozen, D. Abraham, et al., *Phys. Rev. Lett.* **109**, 240505 (2012).
- [30] J. M. Chow, A. Corcoles, J. M. Gambetta, C. Rigetti, B. Johnson, J. A. Smolin, J. Rozen, G. A. Keefe, M. B. Rothwell, M. B. Ketchen, et al., *Phys. Rev. Lett.* **107**, 080502 (2011).
- [31] P. Leek, S. Filipp, P. Maurer, M. Baur, R. Bianchetti, J. Fink, M. Göppl, L. Steffen, and A. Wallraff, *Phys. Rev. B* **79**, 180511 (2009).
- [32] J. Majer, J. M. Chow, J. M. Gambetta, J. Koch, B. R. Johnson, J. A. Schreier, L. Frunzio, D. I. Schuster, A. A. Houck, A. Wallraff, et al., *Nature* **449**, 443 (2007).
- [33] P. Rebentrost and F. K. Wilhelm, *PRB* **79**, 060507(R) (2009).
- [34] J. M. Gambetta, F. Motzoi, S. T. Merkel, and F. K. Wilhelm, *Phys. Rev. A* **83**, 012308 (2011).
- [35] F. Motzoi and F. K. Wilhelm, *Phys. Rev. A* **88**, 062318 (2013).
- [36] R. Schutjens, F. A. Dagga, D. Egger, and F. Wilhelm, *Phys. Rev. A* **88**, 052330 (2013).
- [37] C. Quintana, K. Petersson, L. McFaul, S. Srinivasan, A. Houck, and J. Petta, *Phys. Rev. Lett.* **110**, 173603 (2013).
- [38] S. E. Economou and E. Barnes, *Phys. Rev. B* **91**, 161405 (2015).
- [39] E. Barnes and S. Das Sarma, *Phys. Rev. Lett.* **109**, 060401 (2012).
- [40] E. Barnes, *Phys. Rev. A* **88**, 013818 (2013).
- [41] L. H. Pedersen, K. Molmer, and N. M. Moller, *Phys. Lett. A* **367**, 47 (2007).
- [42] See Supplemental Material for details.